Electronic Supplementary Material (ESI) for New Journal of Chemistry.

Supporting information

Influence of hollow sphere surface heterogeneity and geometry of N-doped carbon on sensitive monitoring of acetaminophen in human fluids and pharmaceutical products

M.Y. Emran[a,b], E. Talat[c], S.A. El-Safty[a*], M.A. Shenashen[a], E.M. Saad[c*]

[a] National Institute for Materials Science (NIMS), 1-2-1 Sengen, Tsukuba-shi, Ibaraki-ken, Japan

[b] Department of Chemistry, Faculty of Science, Al-Azhar University, Assiut 71524, Egypt

[c] Department of Chemistry, Faculty of Science, Suez University

[*]Corresponding author (S.A. El-Safty): sherif.elsafty@nims.go.jp

[*]Corresponding author (E.M. Saad): eman.mohamed@sci.suezuni.edu.eg

1. Experimental

1.1 Chemicals

All chemicals used were of analytical grade or the highest purity available. Sodium phosphate dibasic and monosodium phosphate, ascorbic acid, tryptophan, glucose, adrenaline, noradrenaline, acetaminophen and dopamine were purchased from Sigma-Aldrich company. Lactose, sodium hydroxide, sodium lauryl sulfate, urea, sodium chloride, and HCLwere purchased from el-gomhouria company-Egypt https://el-gomhouria.com/. Pharmaceutical Cetal tablets were purchased from drug stores (Epico- Egypt). Human serum was purchased from Sigma-Aldrich company https://www.sigmaaldrich.com/european-export.html. Human urine samples was collected from volunteer under certificate of approval from scientific ethics committee of Faculty of Science, Al-Azhar University, Assiut, Egypt.

1.2 Electrochemical cells and instrumentation

Electrochemical measurements were carried out by using a Potentiostat /Galvanostat Model 273A. A voltammetric cell with three electrodes was used: a glassy carbon electrode as a working electrode (WE), a platinum electrode as the counter electrode (CE), and an Ag/AgCl/Cl^- (3 mol L^{-1}) as the reference electrode (RE). The electrochemical measurements were done via an

electrochemical impedance analyzer potentiostat (model PGZ 100, Eco Chemie B.V, Utrecht, Netherlands) driven by the general-purpose electrochemical system data processing software (Voltalab Master 4 software).

1.3 Characteristic techniques

Field-emission scanning electron microscopy (FE-SEM) images and EDX-SEM mapping were obtained using a JEOL JEM-7100 (Jeol High-Tech. Co.). Raman shift spectroscopy (HR Micro Raman spectrometer, Horiba, Jobin Yvon) was conducted using an Arion laser at 532 nm. X-ray diffraction (XRD) results were recorded by powder pattern scanned in Philips X'pert Pro Powder diffractometer using Cu Ka radiation with the operating voltage 40 kV and current 20 mA. The surface properties of the material involving the pore structure distribution and surface area were estimated by N_2 adsorption-desorption isotherms at 77 K using a BELSORP36 analyzer (JP. BEL Co., Ltd.). The specific surface area (S_{BET}) was calculated using the Brunauer–Emmett–Teller (BET) method with multipoint adsorption data from the linear section of the N_2 adsorption isotherm. The pore size distribution was determined using nonlocal DFT (NLDFT). A pH-meter sensION™, (pH31) was used for pH adjustment. The XPS analysis was conducted on a PHI Quantera SXM (ULVAC-PHI) instrument (Perkin–Elmer Co., USA) equipped with Al Kα as an X-ray source for excitation (1.5 mm × 0.1 mm, 15 kV, 50 W) under a pressure of 4 × 10−8 Pa. A thin film of the sample was deposited on a Si slide before the start of analysis.

2. Results and discussion

XPS -analysis of N-HCCS

The XPS analysis of N-HCCS illustrates the atomic contents and functional groups. Three peaks centered at 285, 531, and 391 eV are observed and related to C, O, and N, respectively (Figure S2A). The XPS survey of N 1s illustrates four main peaks centered at 398.22, 399.14, 400.4, and 402.6 eV (Figure S2C). These peaks were related to the presence of pyridinic nitrogen (C=N), pyrrolic nitrogen (C–N), graphitic nitrogen, and N-oxide of pyridinic nitrogen or oxidized nitrogen, respectively. The C1s spectrum illustrated the presence of 285.01, 285.8, 288.2, and 289.4 eV peaks that matched with C–C (sp^2), C–C (sp^3), C=O, and O–C=O bands, respectively (Figure S2D). Furthermore, the

high resolution of the XPS for O 1s was performed in the range of 525–540 eV, where three peaks were observed, as shown in Figure S2B. The peaks were assigned to the isolation of –OH/–C=O, which was in 531.4 eV, and the peak at 532 was due to the C=O, whereas the peak at 533.4 was attributed to the contributions of O–C–O, C–O–OH and C–OH. These results confirm the formation of N-doped carbon materials.

Figures and Tables

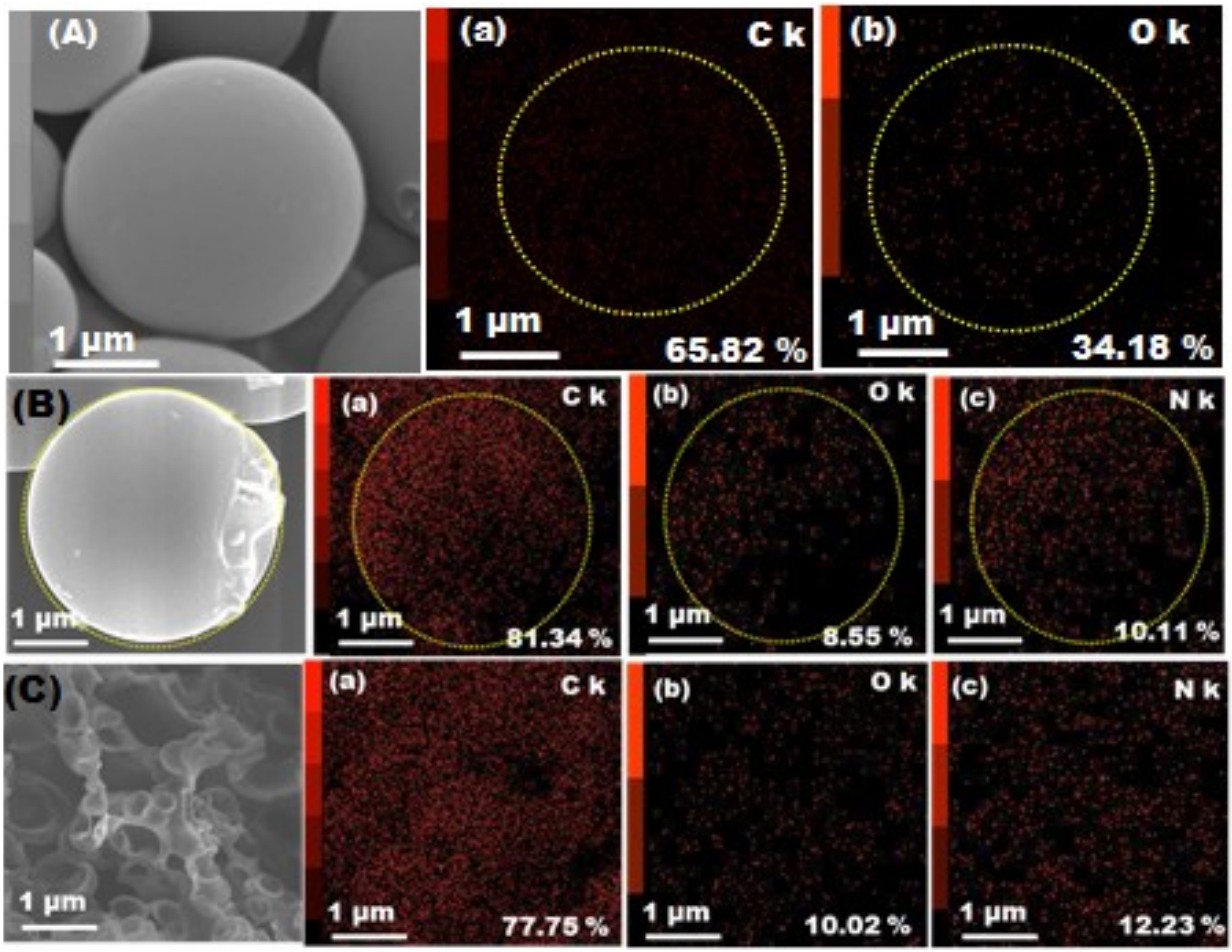

Figure S1. A) The EDX-mapping of CMS for C (a) and O (b). B) The EDX-mapping of N-CSB for C (a), O (b), and N (c). C) The EDX-mapping of N-HCCS for C (a), O (b), and N (c).

Table S1. The EDX-mapping of various %C, %O, and %N of CMS N-CSB, and N-HCCS

Material	Elemental composition, %		
	% C	% O	% N
CMS	65.82	34.18	-
N-CSB	81.34	8.55	10.11
N-HCCS	77.75	10.02	12.23

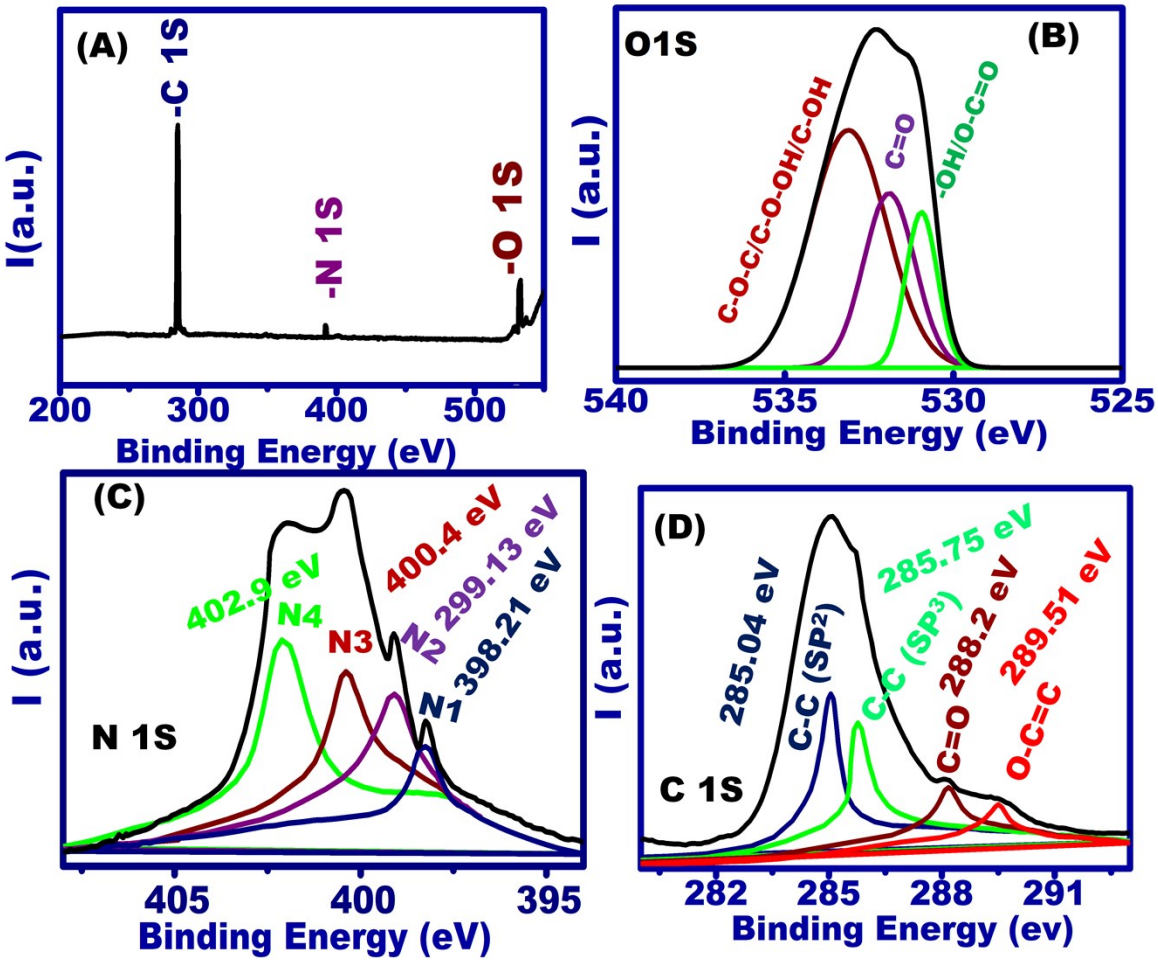

Figure S2. A) The XPS spectrum of N-HCCS. The XPS survey of O 1S (B), N 1S (C), and C 1S (D)

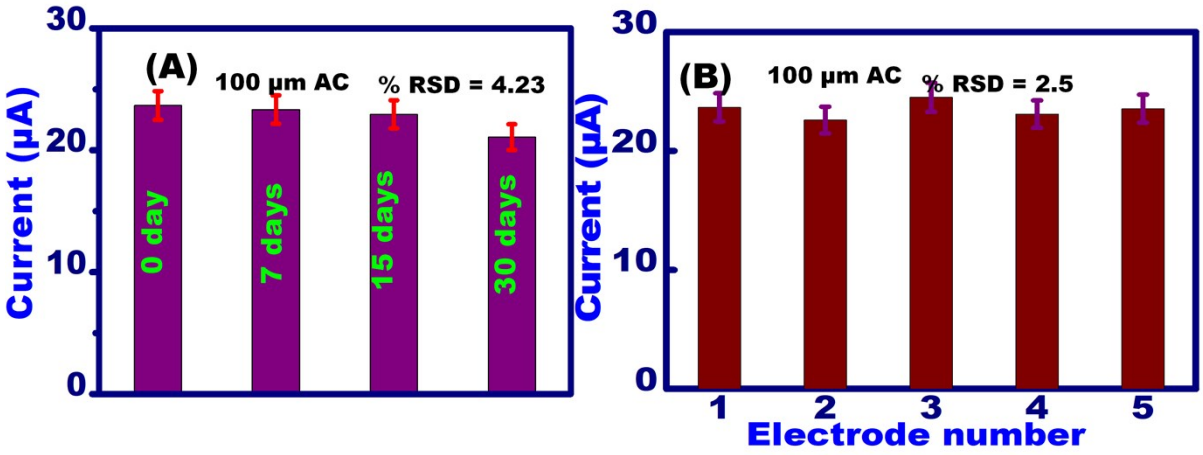

Figure S3. A) the stability studies after using the same electrode of N-HCCS/GCE for several days in the same concentration of 100 µM AC (pH = 6.4). B) The N-HCCS/GCE reproducibility after designing 5 electrodes in 100 µM AC (pH = 6.4).

Table S2. Survey of AC detections using different modified electrodes obtaining the limit of detection and linear range, and the detection limit of N-HCCS with its linear range.

Electrode	AC		Ref.
	Linear range (µM)	**The detection limit (µM)**	
PCA@ Zn/Ni-ZIF-8–800/GCE[a]	0.00 –1000	0.0291	[1]
Co-NCNHP/GCE[b]	0.1 – 500	0.05	[2]
ERG/Ni2O3–NiO/ GCE[c]	0.04 – 100	0.02	[3]
Fe_3O_4@SiO_2-free-MIP/MCPE[d]	0.6 – 50	0.017	[4]
Halloysite nanotubular clay/GCE	0.06 –14	0.011	[5]
Yb_2O_3 NP /CPE[e]	0.25 – 654	0.055	[6]
GA@O-CQDs[f]	0.1 – 10	0.38	[7]
N-HCCS/GCE	10 – 800	0.08	This work

[a] Poly caffeic acid (PCA) @ Zn/Ni-ZIF-8–800

[b] Cobalt-nitrogen co-doped carbon nanotube hollow polyhedron

[c] Electrochemically reduced graphene/ nickel oxides /glassy carbon electrode

[d] Molecularly imprinted membrane (MMIP)@ Fe_3O_4@SiO_2 NPs/carbon paste electrode

[e] Yb_2O_3 nanoplates (NPs) /carbon paste electrode

[f] Graphene aerogel@octadecylamine-functionalized carbon quantum dots

Table S3: Determination of AC in human blood serum samples was carried out by spiking various AC concentrations in the range of 10-150 µM on the N-HCCS-modified electrode. The standardization analyses of targets were determined according to SWV techniques and repeated 3 times per each sample analysis. Not C_A is a concentration of target molecules, C_F is the concentration founded for the molecules, and %R is the percentage of recovery (%R= C_F/C_A x 100), respectively.

Targets	C_A /µM	C_F /µM	% R
AC	10	9.98 ± 0.001	99.8
	50	49.6 ± 0.004	99.2
	100	99.4± 0.006	99.4
	150	148.6 ± 0.007	99.06

Table S4: Determination of AC in the human urine sample was carried out by spiking various AC concentrations in the range of 10 -300 μM on N-HCCS-modified electrode. The standardization

Targets	C_A /μM	C_F /μM	% R
AC	10	9.99 ± 0.001	99.9
	50	49.56 ± 0.004	99.12
	100	99.59 ± 0.006	99.59
	150	148.2± 0.007	98.8
	200	198.4± 0.002	99.2
	250	249.8± 0.001	99.92
	300	298.6 ± 0.003	99.53

analyses of targets were determined according to SWV techniques and repeated 3 times per each sample analysis. Not C_A is a concentration of target molecules, C_F is the concentration founded for the molecules, and %R is the percentage of recovery (%R= C_F/C_A x 100), respectively

References

1. W. Zhang, S. Liu, Y. Zhang, X. Ding, B. Jiang and Y. Zhang, *Biosensors and Bioelectronics*, 2019, **131**, 200-206.
2. Y. Jin, X. Li, C. Ge, J. Ma, Y. Li, E. Zhao, S. Yao, G. Xu and D. Li, *Microchimica Acta*, 2020, **187**, 6.
3. G.-T. Liu, H.-F. Chen, G.-M. Lin, P.-p. Ye, X.-P. Wang, Y.-Z. Jiao, X.-Y. Guo, Y. Wen and H.-F. Yang, *Biosensors and Bioelectronics*, 2014, **56**, 26-32.
4. C. Su, Z. Li, D. Zhang, Z. Wang, X. Zhou, L. Liao and X. Xiao, *Biosensors and Bioelectronics*, 2020, **148**, 111819.
5. J. Kalaiyarasi, S. Meenakshi, S. C. Gopinath and K. Pandian, *Microchimica Acta*, 2017, **184**, 4485-4494.
6. M. Khairy and C. E. Banks, *Microchimica Acta*, 2020, **187**, 126.
7. L. Ruiyi, Z. Haiyan, L. Zaijun and L. Junkang, *Microchimica Acta*, 2018, **185**, 145.